

TEST TECHNIQUE FOR CHECKING THE FORWARD MOTION
COMPENSATION DEVICE IN THE LMK AERIAL SURVEY
CAMERA SYSTEM

Verm.-Ing. Ulrich Zeth and Dipl.-Phys. Norbert Dietsch
Kombinat VEB Carl Zeiss JENA
GDR

Commission I/5

General considerations of the effect of image motion

It should be undisputed today that the use of forward motion compensators in modern aerial mapping cameras is of great advantage. Only these compensators make it possible to reproduce the high imaging quality of the camera lenses, which can be proved with high-resolution and hence relatively insensitive aerial films under laboratory conditions, without substantial restrictions also under flying conditions with the same aerial films. Forward motion compensators thus have a decisive influence on the efficiency of the overall photogrammetric process.

It is obvious from the modulation transfer function of the mainly involved transfer components (Fig. 1) that the imaging quality is most drastically influenced by forward motion. While the MTF curves of lens and film behave asymptotically, the MTF curves of forward image motion irresistibly approach zero and thus finally determine the limiting resolution of the entire system. This fact is only slightly alleviated by the circumstance that because of the film response threshold the image motion amount being considered here becomes not fully effective photographically (generally the theoretically calculated amount is used). The image blur caused by forward motion is additionally superposed by effects resulting from lens shutter efficiency, the size of image motion itself, and other boundary conditions such as object contrast and development. Consequently, as shown in Fig. 2 by the

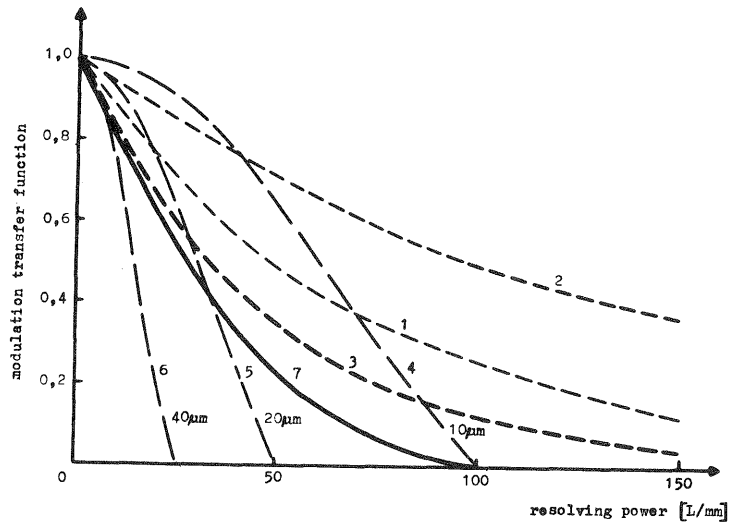


Figure 1 Influence of image motion on image quality, represented by the modulation transfer functions (MTF) of lens, film and image motion
 1 AWAM lens (AWAM = Area Weighted Average Modulation transfer)
 2 MTF film
 3 MTF lens + film
 4-6 MTF image motion
 4 for $\Delta e' = 10 \mu\text{m}$
 5 for $\Delta e' = 20 \mu\text{m}$
 6 for $\Delta e' = 40 \mu\text{m}$
 7 resultant MTF for lens + film + image motion $\Delta e' = 10 \mu\text{m}$

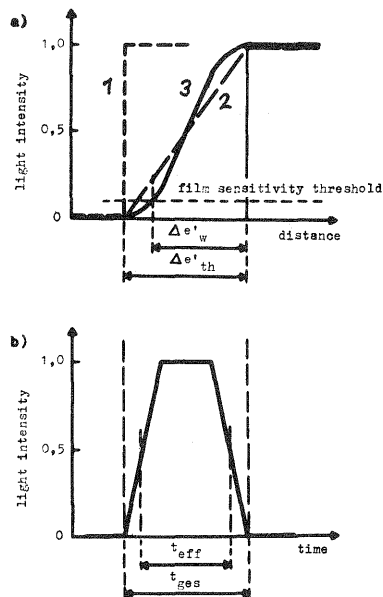


Figure 2 a) Image blur owing to forward motion represented by the shift of intensity distribution at an edge
 1 Intensity distribution in case of static exposure
 2 Intensity distribution in case of forward motion by the amount $\Delta e'$ on exposure with an ideal shutter (100% efficiency)
 3 Intensity distribution of the really imaged, blurred edge on exposure with a common shutter (efficiency about 70%)
 b) Efficiency of a common between-lens shutter

example of the image of an edge, the edge is not only shifted because of image motion but additionally deformed by the irregular intensity distribution due to the shutter efficiency, so that the edge becomes steeper in the middle range. Its lower part drops into an intensity range which lies below the response threshold of the emulsion. This reduces the effective amount of blur $\Delta e'_w$ compared to the theoretical amount $\Delta e'_{th}$ by about 20% in our example. For better understanding, Figure 2b shows the temporal intensity behaviour caused by the shutter as a function of efficiency, with the magnitude of the total exposure time t_{ges} corresponding to the theoretical amount of blur $\Delta e'_{th}$ in Fig. 2a because of the existing relationship between the two parameters.

The size of the image motion amount itself has such an effect that with increasing image motion the curves presented in Fig. 2a are further flattening, so that their portion lying below the response threshold of the film increases. Fig. 3 shows the results of the relevant investigations made on the image motion simulator (description see below). In the range from $\Delta e'_{th} = 5$ to $130 \mu m$ the theoretically derived image motion amounts $\Delta e'_{th} = v_{image} \cdot t$ are shown as a function of the measured blur amounts $\Delta e'_w$ in the image being effective at the test squares and a mean curve (C) derived from this is recorded.

Here it is noteworthy that unlike Fig. 2a where the relationship between image motion amount $\Delta e'_{th}$ and blur amount $\Delta(e')_w$ is shown for one edge, the blur amount is further reduced for an object bounded by two edges, in this case the test square, since the "ineffective" difference amount $\Delta e'$, with equal size of the image motion amount, occurs on both edges.

The seemingly plausible assumption that the reduction is proportional to the size of the image motion amount, for example according to the theoretically derived curve (B), was not corroborated. In the investigations it was found that up to a theoretical image motion of about $10 \mu m$ a blur of the

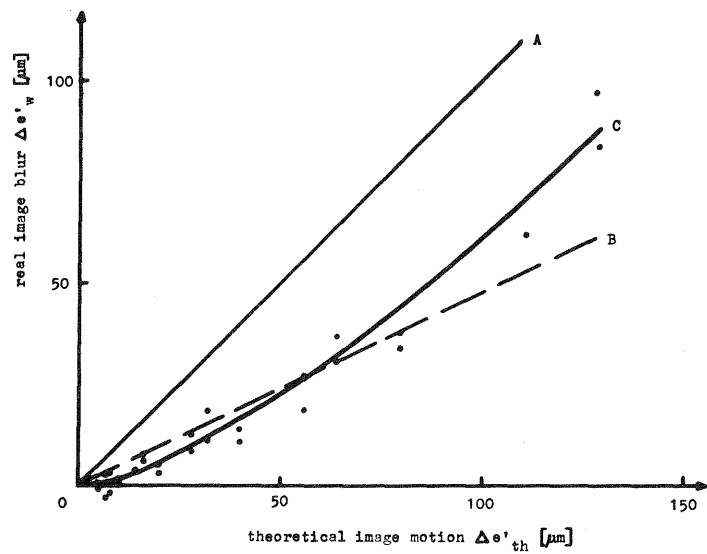


Figure 3 Image blur in dependence on the size of the amount of image motion

A $\Delta e'_{\text{image}} = \Delta e'_{\text{th}}$
 B Size of image blur (theoretical derivation)
 C Size of image blur (experimentally determined)

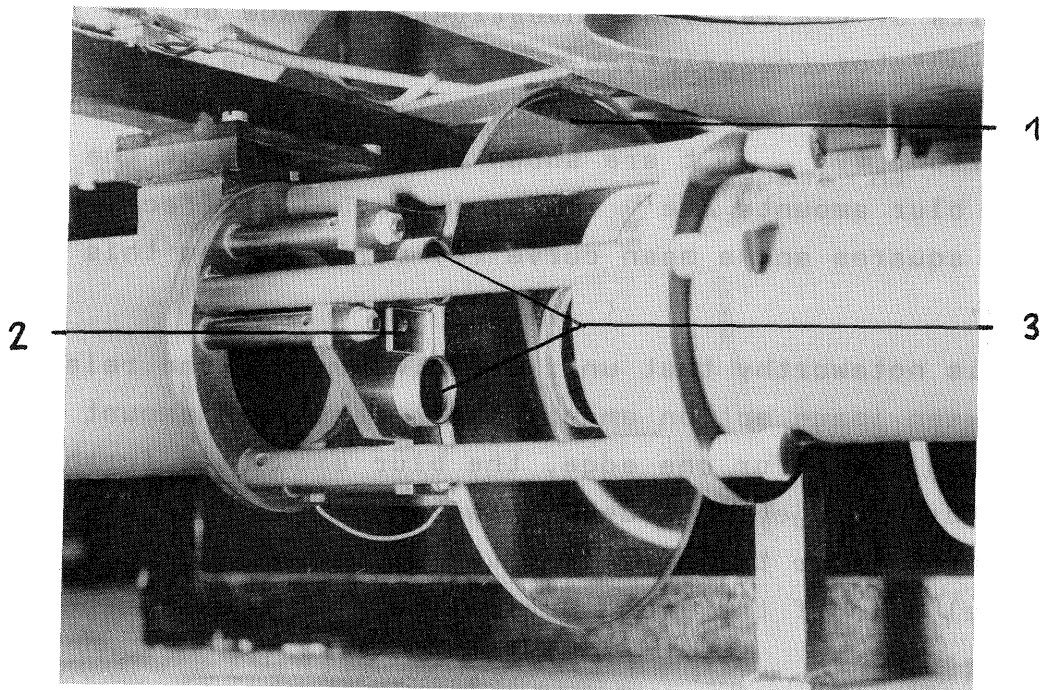


Figure 4 Test pattern in the focal plane of the forward motion simulator

1 Motion test disc
 2 Stationary test object
 3 Fixtures of the resolution test

contours could practically not be noticed; deviating measurement results lie within the measuring uncertainty and are more or less induced by it. If a practically effective image blur of $\leq 10 \mu\text{m}$ is still tolerated, then on the basis of the result of these investigations the 3-fold value can be assumed as image motion amount. In the further behaviour of the curve this factor is decreasing and from about $\Delta e'_{th} = 100 \mu\text{m}$ the curve suggests a constant reduction of the theoretical image motion amount by about $40 \mu\text{m}$. However, this is already a region that in the consideration of the image motion as error influence lies outside the discussion. The present investigations were made using the test square in the motion test of the image motion simulator (Fig. 5), i.e. a test object with high object contrast. As already mentioned, other influences not investigated here result from a changed object contrast and from different development conditions.

Forward motion compensation and its testing

As to the LMK Aerial Survey Camera, forward motion compensation was introduced already in 1983. It is implemented in the following way: At the moment of exposure the film held flat by vacuum against the platen is moved in flying direction at a speed resulting from the V/H ratio (velocity of the aircraft over the ground to the height over the terrain) $/1, 2/$. From the above it becomes obvious that the realization of the complicated, partially overlapping motion phases involved requires high accuracy. As shown in Figure 1, a loss of imaging quality with modern high-performance lenses due to forward motion can only be avoided, if the residual errors in the image occurring in case of compensation are kept below $10 \mu\text{m}$. This applies to the guiding accuracy as well as the motion accuracy of the film platen and the film adhering to it. On the other hand, the mentioned differences between the theoretically calculated image motion amount and the actual effect in the image show that it is advisable in quality inspection to use testing devices and methods which largely correspond to practical operation conditions or

which allow an analysis of the film motion phases in the image plane.

The following report deals with such test methods, which are used for the inspection of all LMK magazines made in Jena.

By means of the "forward motion simulator" we test the speed of compensation, the moment of exposure for the fiducial marks and the film position in the image plane. The forward motion simulator mainly consists of a collimating telescope with folded optical beam and an illumination system of the type as used in our "image quality testing device" for focus adjustment and camera calibration /3/. Thus the requirement is met that the used test image seems to come from infinity.

The depth resolution test used in the image quality testing device is replaced by a rotating chromium-plated glass disc (Fig. 4) having around its periphery test figures in the shape of an "endless" series of transparent squares of high dimensional accuracy (Fig. 5). The rotation centre of the glass disc is arranged eccentrically relative to the collimating telescope, so that the series of square test figures runs through the optical axis of the telescope in its focal plane. By a common control frequency, the rotation speed is coupled with the speed of the travelling grid in the control unit, and thus with the given compensation speed. This arrangement excludes errors in setting the test speeds. The test criterion is that the imaged test figures appear as squares and not as distorted rectangles. Since always both dimensions of the square, viz. width and length, are measured, any possible photographic edge effects (e.g. resulting from inaccurate exposure or development) compensate each other and thus have no influence on the result.

In order to exclude errors resulting from the curved moving direction of the test disc, only those squares are tested which are directly opposite to the stationary test object

(Fig. 5). This test object marks the point on the test disc where the tangent line to the rotating test series is parallel to the compensation direction within the magazine, provided the camera to be tested is appropriately aligned above the telescope.

The checking of the exposure moment of the fiducial marks results from the requirement that this exposure must be made within a few milliseconds at the mid-point of photo exposure in order to guarantee the inner orientation of the lens cone derived from the fiducial mark images (see /2/).

The check is made in the following way: The position of the point of the test object relative to the fiducial marks located right and left in flying direction in an image with forward motion compensation is compared by comparator measurement with the position of test object relative to the fiducial marks in an image without forward motion compensation. In both cases, the geometrical centre of the point of the test object is determined in flying direction in order to avoid errors resulting from image blurring found in the image with compensation. The tolerable position difference between both images amounts to ± 0.01 mm.

The arrangement of resolution tests in the focus of the collimating telescope additionally allows - in photos taken with a stationary camera, i.e. without motion compensation - checks whether the film is held flat by vacuum against the platen, at least for the central area covered by the tests. The same test patterns must be resolved as for the calibration photos with the image quality testing device, provided the same test emulsion is used.

Another test method is used especially for error analysis, which is not readily possible with the forward motion simulator. With the help of a special circuit the fiducial marks are selected and exposed on to the film at a certain clock frequency in the period between "START" and "STOP" of the

compensation movement. Thus multiple images of the fiducial marks appear on the film in the form of a line-and-space grating. From the distances between neighbouring lines of the fiducial mark images one can derive the instantaneous speed of the film at these points.

Figures 6 and 7 demonstrate the described test methods by two examples, with (a) showing the photos taken of test images in the forward motion simulator, (b) showing the fiducial mark line-and-space grating exposed on to the film and (c) showing the appertaining analysis of the line-and-space grating. For better orientation, these curves are provided with marks for times and periods of the extreme shutter speeds $t = 1/30$ s and $t = 1/500$ s. In both examples the shutter speed was $1/30$ s and the cycle time of the fiducial mark exposures was 5 ms. The additional fiducial mark in Figure 6, which is clearly noticeable and marked by an arrow, is the proper fiducial mark image which is correlated to the camera exposure cycle.

Fig. 6 shows a photograph taken at a compensation speed of 64 mm/s. The blurring of the static elements of the test image, viz. test figure and resolution test pattern, clearly indicates the forward motion amount which would appear in a photo taken without compensation ($\Delta e' = v_{\text{image}} \cdot t = 64 \cdot 1/32 = 2$ mm).

The squares of the motion test, however, are sharply imaged as undistorted squares within the above-specified test area. Deformation of the test squares outside the test area is caused by the curved moving direction of the test series. The analysis of the fiducial mark line-and-space grating shows, just as the grating itself owing to its equal spacings, the exact adherence to the given compensation speed throughout the full exposure range.

It can be seen that even an exposure with $t = 1/500$ s would be correctly compensated, although made immediately after the start of the compensation movement, since the latter attains the preselected speed very quickly.

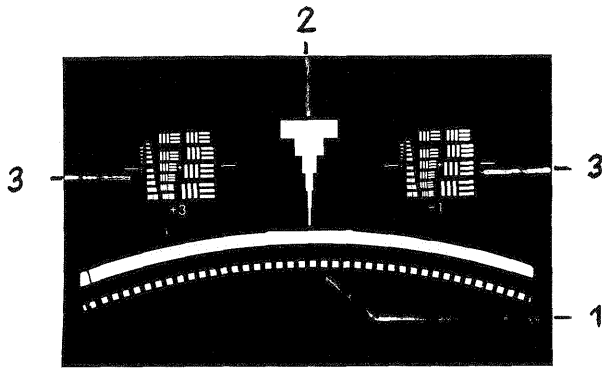


Figure 5 Test image of the forward motion simulator
 1 Section of the motion test with test squares
 2 Stationary test object
 3 Resolution tests

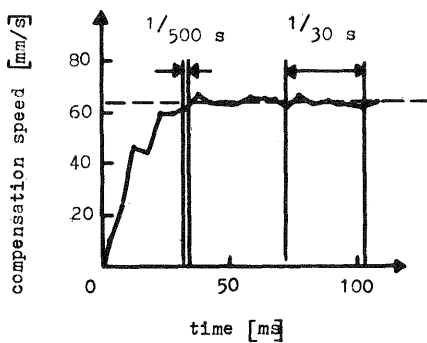
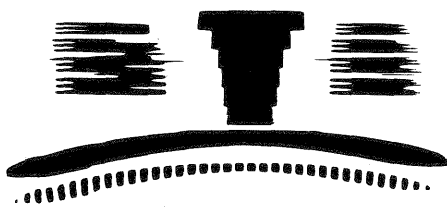


Figure 6 Test photograph and analysis (description see text)

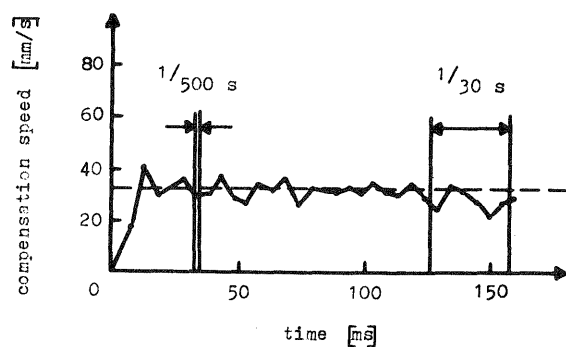
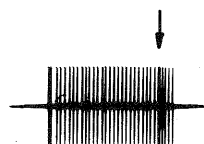
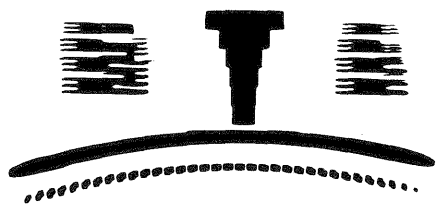


Figure 7 Test photograph and analysis (description see text)

Just for demonstration, Figure 7 shows an example of an incomplete compensation from a test series. It is evident from the analysis of the fiducial mark line-and-space grating that the error is caused by a decrease of the compensation speed within the exposure period below the nominal value.

Also in the remaining range the compensation speed shows some irregularities.

The use of the forward motion simulator in the factory inspection of LMK magazines ensures a consistently high quality of this important camera function.

REFERENCES

- /1/ Voss, G.; Zeth, U.: Das Aufnahmesystem Luftbildmeßkammer LMK, eine neue Generation von Luftbildmeßkammern aus Jena (The LMK Aerial Camera System, a new generation of aerial cameras from Jena). Vermessungstechnik, Berlin 31(1983)3, pp. 78 -80; Sensing the Earth, Jena (1984)2, pp. 12 - 14; Kompendium Photogrammetrie Vol.16(1983) pp. 25 - 31; Int. Archiv f. Photogrammetrie und Fernerkundung, Rio de Janeiro 25(1984)1, pp. 314 - 319
- /2/ Zeth, U.; Voss, G.: Einige Aspekte zur Linearbildwanderungskompensation im Aufnahmesystem Luftbildmeßkammer LMK (Some aspects of forward motion compensation in the LMK aerial survey camera system). Vermessungstechnik, Berlin 31(1983)9, pp. 293 - 298; ASP-March Meeting, Washington 1983; Sensing the Earth, Jena (1984)2, pp. 14 - 20; Int. Archiv f. Photogrammetrie und Fernerkundung, Rio de Janeiro 25(1984)1, pp. 339 - 350; Kompendium Photogrammetrie Vol. 17(1985) pp. 17 - 32
- /3/ Würtz, G.: Prüfung und Kalibrierung von Luftbildmeßkammern in Jena. Kompendium Photogrammetrie Vol. 7(1966) pp. 7 - 28